DOI: 10.26599/FSHW.2026.9251058

Contents lists available at SciOpen

Food Science and Human Wellness

journal homepage: https://www.sciopen.com/journal/2097-0765

China Food Publishing Co.

The potential immunomodulatory mechanism of fucoidan, a heteropolysaccharide from *Sargassum hemiphyllum* through TNF and IL-17 signaling pathways based on RNA-seq

Qing-Ling Zhou[a,1], Xiao-Fei Liu[a,1], Kun Yang [a], Zhuo Wang[a], Bing-Bing Song[a], Qiao-Li Zhao[a], Xue-Jing Jia[a], Cheong Kit Leong[a], Sai-Yi Zhong[a,b]*, Rui Li[a,]*

[a] *College of Food Science and Technology, Guangdong Ocean University, Guangdong Provincial Key Laboratory of Aquatic Product Processing and Safety, Guangdong Province Engineering Laboratory for Marine Biological Products, Guangdong Provincial Engineering Technology Research Center of Seafood, Guangdong Provincial Engineering Technology Research Center of Prefabricated Seafood Processing and Quality Control, Guangdong Provincial Science and Technology Innovation Center for Subtropical Fruit and Vegetable Processing, Zhanjiang 524008, China*

[b] *Shenzhen Research Institute, Guangdong Ocean University, Shenzhen 518108, China*

ABSTRACT: The crude fucoidan extracted from *Sargassum hemiphyllum* (*S. hemiphyllum*) demonstrated notable immunomodulatory effects; however, its structural features and mechanistic underpinnings remained poorly understood. In this study, the crude polysaccharide from *S. hemiphyllum* (F) was purified to yield a product named FS, its molecular characteristics, thermal properties, and microscopic morphology were systematically examined, alongside its immunomodulatory mechanisms. The main monosaccharide components of F were fucose (22.80%), galactose (15.40%), glucuronic acid (15.95%), and mannuronic acid (14.40%), while FS were primarily composed of fucose (23.00%), mannose (13.39%), xylose (12.36%) and glucuronic acid (24.24%). All three polysaccharides exhibited favorable thermal stability. Immunostimulation assays indicated that FS significantly promoted the secretion of cytokines—TNF-α, IL-1β, and IL-6 in RAW264.7 macrophages. RNA sequencing analysis further identified 501 differentially expressed genes after FS treatment, comprising 206 up-regulated and 295 down-regulated genes. Mechanistic studies revealed that FS mediates immunomodulation mainly via activation of the TNF/IL-17 signaling pathway. These findings offer new perspectives on the immunomodulatory mechanisms of marine polysaccharides and provide a critical theoretical foundation for their application in functional foods and nutritional supplements.

Keywords: brown algae; marine polysaccharide; fucoidan; immunomodulatory mechanism; RNA-seq

1. Introduction

The development of numerous diseases is closely associated with dysfunctions of the body's immune system. Maintaining a proper balance between the innate and adaptive immune responses is therefore essential for immune homeostasis. As the first line of defense, the innate immune system plays a critical role in mounting initial protective response. Dysregulation of this system may lead to autoimmune disorders[1], while impaired immune function can increase susceptibility to infections and cancers. Current immunomodulatory

***Corresponding author**
Rui Li, lirui@gdou.edu.cn; Sai-Yi Zhong, zhongsy@gdou.edu.cn

Received 26 September 2025
Received in revised from 30 October 2025
Accepted 2 December 2025

therapies, such as sulfasalazine and diclofenac, are often associated with adverse effects including nausea, vomiting, dizziness, and headache, largely due to their synthetic nature and non-specific modes of action[2]. These limitations have spurred interest in identifying novel immunomodulators from natural sources that offer improved safety profiles and minimal side effects. Recent advances in immunotherapy have demonstrated significant potential in modulating specific immune responses[3]. This progress has accelerated the exploration of various immunomodulatory agents, particularly those derived from natural sources. As Li et al. pointed out, natural products, as a valuable source of active ingredients, it is a feasible strategy to develop immunomodulators from natural products[4].

In recent years, seaweed-derived polysaccharides have gained extensive attention for their applications in the food, pharmaceutical, cosmetic, and feed industries[5]. These bioactive compounds are valued for their natural availability, favorable safety, and biodegradability[6]. Notably, sulfated polysaccharides from seaweeds exhibit a broad spectrum of biological activities, including antioxidant[7], anti-inflammatory[8], anticancer[9], antidiabetic[10], gut microbiota-modulating[11], antibacterial[12], and immunomodulatory effects[13]. The bioactivity of these polysaccharides is closely influenced by structural features such as sulfation patterns, monosaccharide composition, and branching complexity[14]. A detailed understanding of their physicochemical and biological properties is essential for advancing the high-value utilization of seaweed polysaccharides.

Sargassum hemiphyllum (S. hemiphyllum), a brown algae prevalent in the warm waters of the northwestern Pacific Ocean[15], is a promising source of bioactive polysaccharides. Previous studies on polysaccharides from *S. hemiphyllum*, have reported antitumor[16], anti-inflammatory[17], and neuroprotective activities[18]. Our earlier work indicated that crude polysaccharides from this seaweed exhibit immune-enhancing potential[19]. However, further purification and detailed mechanistic studies are necessary to elucidate the specific immunomodulatory pathways involved.

Sulfated polysaccharides from seaweeds have shown considerable promise in modulating immune responses across various contexts, including autoimmune diseases[20], allergic conditions[21], and immunodeficiency disorders[22]. Classical immune pathways such as nuclear factor kappa B (NF-κB) and mitogen-activated protein kinase (MAPK) are frequently implicated—for instance, low-molecular-weight polysaccharides from *Undaria pinnatifida* activate both pathways[23], and similar mechanisms are observed in sulfated polysaccharides from *Cystoseira indica*[24] and *Caulerpa chemnitzia*[25]. Beyond these, the IL-17 signaling pathway represents another pivotal immunoregulatory axis, primarily involved in inflammation and host defense through binding of cytokines such as IL-17A and IL-17F[26].

Despite these advances, the immunomodulatory properties and mechanisms of purified fucoidan from *S. hemiphyllum* remain unexplored. Therefore, this study aimed to extract, purify, and characterize fucoidan from *S. hemiphyllum* through ultrasonic-assisted hot water extraction, column chromatography, and Fourier-transform infrared spectroscopy (FTIR). The purified fucoidan was further evaluated for its effects on RAW264.7 macrophage viability, NO production, as well as the secretion and gene expression of key

pro-inflammatory cytokines including interleukin-1β (IL-1β), interleukin-6 (IL-6), and tumor necrosis factor-α (TNF-α). Additionally, transcriptomic analysis was conducted to elucidate the underlying immunomodulatory mechanisms. To our knowledge, this is the first study to investigate the immunoregulatory effects of purified *S. hemiphyllum* fucoidan and its possible involvement of the IL-17 signaling pathway, providing new insights into its potential as an immunostimulatory agent.

2. Materials and methods

2.1 Materials

S. hemiphyllum was harvested in March 2023 off the coast of Naozhou Island, Zhanjiang, Guangdong Province, China. DEAE-cellulose 52 was purchased from Yuanye Biotechnology Co., Ltd. (Shanghai, China), and Sephacryl S-300 was obtained from Solarbio Science and Technology Co., Ltd. (Beijing, China). RAW264.7 macrophage was supplied by Procell Biotechnology Co., Ltd. (Hubei, China). The CCK-8 assay kit was sourced from Biosharp Biotechnology (Beijing, China). Lipopolysaccharide (LPS) and NO assay kits were provided by Beyotime Biotechnology (Shanghai, China). Cytokine ELISA kits were purchased from Enzyme Immunoassay Industry Co., Ltd. (Jiangsu, China). Fetal bovine serum (FBS) and Dulbecco's modified eagle medium (DMEM) were purchased from Gibco Life Technologies (Grand Island, NY, USA). RAW264.7 macrophages were purchased from Wuhan Pricella Biotechnology Co., Ltd. (Wuhan, China). All other chemicals were of analytical grade.

2.2 Extraction, isolation, and purification of polysaccharides

Crude polysaccharide was extracted following a modified version of our previously described method[27]. Briefly, 30 g of *Sargassum* powder was mixed with 900 mL of deionized water and subjected to ultrasonic treatment at 350 W for 50 min. The mixture was then stirred magnetically and extracted at 80 °C for 3.5 h. The extract was concentrated to a quarter of its original volume using a rotary evaporator, after which anhydrous ethanol was added to a final concentration of 30% (v/v). The resulting supernatant was further mixed with four volume of anhydrous ethanol. To remove proteins, Sevag reagent was added at a ratio of 6:1, and the process was repeated five times. The supernatant was dialyzed in a 3500 Da molecular weight cutoff dialysis bag against distilled water at 4 ºC for 48 h, with water changed three times, the retentate was freeze-dried to obtain the crude polysaccharide, designated as F.

For further purification, 200 mg of crude polysaccharide F was redissolved in 10 mL deionized water and carefully loaded onto a DEAE-52 cellulose column (26 mm × 600 mm). The column was equilibrated and eluted stepwise with 1 L of NaCl solutions (0, 0.5, 1.0, and 1.5 mol/L) at a flow rate of 1 mL/min. The resulting fractions were labeled FD1, FD2, and FD3, respectively. Each fraction was concentrated and dialyzed against deionized water using a 3500 Da dialysis membrane for 48 h, then freeze-dried. The fraction with the highest yield, FD2, was further purified by elution on a Sephacryl S-300 column (16 mm × 600 mm) with ultrapure water at a low flow rate of 0.3 mL/min. The purified polysaccharide obtained from this step was named FS and used for subsequent experiments.

2.3 Chemical Composition Analysis

The chemical composition of polysaccharide fractions F, FD2, and FS were analyzed. The polysaccharide content was determined using phenol-sulfuric acid method with L-fucose as a standard[28]. Protein content was measured using a BCA assay kit. Sulfate group content was quantified by barium chloride-gelatin turbidimetry[29], and polyphenol content was assessed using the Folin-Ciocalteu method[30].

2.4 Characterization of Physiochemical Properties

2.4.1 Determination of molecular weight

The absolute molecular weights of polysaccharides F, FD2 and FS were determined by gel permeation chromatography coupled with multi-angle light scattering (GPC-MALS). The system consisted of a U3000 HPLC (Thermo Scientific, CA, USA), a DAWN HELEOS II MALS detector (Wyatt technology, CA, USA), and an Optilab T-rEX differential refractive index detector (Wyatt technology, CA, USA). Sample were prepared at a concentration of 1 mg/mL in 0.1 mol/L $NaNO_3$, filtered through 0.45 μm membranes, and 100 μL of each sample was injected into a column (7.8 mm × 300 mm i.d., Borui Saccharide Biotechnology Co. Ltd.) maintained at 60 ºC. The mobile phase consisted of DMSO with 0.5% LiBr, delivered at a flow rate of 0.3 mL/min. Date were processed using ASTRA 6.1 software.

2.4.2 Analysis of monosaccharide composition

Monosaccharide composition was analyzed by high-performance anion-exchange chromatography with pulsed amperometric detection (HPAEC-PAD) on an ICS 5000+ system (Thermo Fisher Scientific, USA) equipped with a Dionex™ CarboPac™ PA20 column (150 mm × 3.0 mm, 10 μm). Briefly, polysaccharide samples were hydrolyzed with 2 mol/L trichloroacetic acid (TFA) at 121 °C for 2 h. After removal of TFA, the hydrolysates were analyzed by HPAEC-PAD. Monosaccharide were quantified by comparing peak areas against calibration curve derived from standard monosaccharides.

2.4.3 UV and FTIR

Polysaccharides F, FD2, and FS were dissolved in deionized water (0.3 mg/mL), and UV absorption spectra were recorded between 200-600 nm using a UV-1900i spectrophotometry (Shimadzu, Japan). For FTIR detection, each polysaccharide was thoroughly mixed with dried KBr at a 1:100 ratio (w/w), ground, and pressed into transparent pellets. FTIR spectra were acquired in the range of 4000-400 cm^{-1} using a Bruker Tensor 27 spectrometer (Ettlingen, Germany).

2.4.4 Differential scanning calorimetry (DSC) and thermogravimetry (TG)

The thermal properties of polysaccharides F, FD2, and FS were investigated using TG and DSC. Measurements were performed on a DSC/DTA-TG analyzer (Netzsch STA449F3, German). Approximately 5.0 mg of each sample was heated from 20 °C to 800 °C at a rate of 10 °C/min under a constant gas flow of 40 mL/min.

2.4.5 Scanning electron microscopy (SEM)

The microstructural features of polysaccharides F, FD2, and FS were examined using a scanning electron microscope (TESCAN MIRA3, Brno, Czech Republic) opened at an accelerating voltage of 5.0 kV. Samples were mounted on copper stubs with double-sided adhesive tape and sputter-coated with gold under vacuum. Images were acquired at magnifications of 200 × and 1000 ×.

2.5 In vitro immunoreactivity assay of polysaccharides

2.5.1 Cell culture and handling

RAW264.7 macrophages were maintained in high-glucose DMEM supplemented with 10% FBS, 100 μg/mL penicillin, and 100 μg/mL streptomycin at 37°C in a 5% CO_2 atmosphere.

2.5.2 Cell viability assay

RAW264.7 cells were seeded into 96-well plates at a density of 1×10^5 cells/mL and cultured for 24 h. The medium was then replaced with 100 μL of fresh medium containing polysaccharide solutions at various concentrations (6.25, 25, 100, and 200 μg/mL). Cells treated with 1 μg/mL LPS, and untreated cells (DMEM only) were used as positive and blank controls, respectively. After 24 h of incubation, the medium was aspirated, and 100 μL of DMEM containing 10% CCK-8 solution was added to each well. Following incubation at 37°C for 1 h, the absorbance at 450 nm was measured using a microplate reader (Thermo Scientific Varioskan LUX, USA).

2.5.3 Assay of NO production

RAW264.7 cells were seeded in 96-well plates at a density of 2×10^5 cells/mL and cultured for 24 h. Then, the medium was replaced with 100 μL of different concentrations of polysaccharide solutions, LPS (1 μg/mL) or DMEM alone. After 24 h of incubation, 50 μL of culture supernatant using the Griess reaction according to the manufacturer's instructions (NO assay kit) and quantified by reference to a sodium nitrite standard curve.

2.5.4 Cytokine assay

RAW264.7 cells were seeded into 24-well plates at a density of 2×10^5 cells/mL and incubated for 24 h at 37 °C. The supernatant was carefully aspirated, and each well was treated with 500 μL of polysaccharide solutions at different concentrations (6.25, 25, 100, and 200 μg/mL). LPS (1 μg/mL) and DMEM alone were used as positive and blank controls, respectively. After incubation, the supernatant was collected, and the levels of TNF-α, IL-6, and IL-1β were measured using commercial ELISA kits according to the manufacturer's instructions.

2.5.5 RT-qPCR

RAW264.7 cells were seeded in 6-well plates at 1×10^6 cells/mL per well and treated with polysaccharide solutions (6.25, 25, and 100 μg/mL), LPS (1 μg/mL), or DMEM alone for 24 h, following the same treatment protocol as previously described. After treatment, cells were collected by centrifugation. Total RNA was extracted using an RNA extraction kit, and cDNA was synthesized by reverse transcription. The primer sequences used are listed in Table 1. GADPH was used as the internal reference gene for normalization. Quantitative PCR was performed using ChamQ Universal SYBR qPCR Master Mix (Vazyme

Biotech Co., Ltd, China) on a Bio-Rad CFX96 Touch real-time PCR system. The relative mRNA expression levels were calculated using the $2^{-\triangle\triangle Ct}$ method.

Table 1. PCR primer sequences.

Gene	Primer sequence（5′→3′）
IL-1β	Forward (F): TCGCAGCAGCACATCAACAAGAG
	Reverse (R): AGGTCCACGGGAAAGACACAGG
IL-6	F: CTTCTTGGGACTGATGCTGGTGAC
	R: AGGTCTGTTGGGAGTGGTATCCTC
TNF-α	F: GTGCCTATGTCTCAGCCTCTTCTC
	R: TGGTTTGTGAGTGTGAGGGTCTG
iNOS	F: ACTCAGCCAAGCCCTCACCTAC
	R: TCCAATCTCTGCCTATCCGTCTCG
COX-2	F: GGTGCCTGGTCTGATGATGTATGC
	R: GGATGCTCCTGCTTGAGTATGTCG
Lcn2	F: GCTACAATGTCACCTCCATCCTG
	R: ATACCTGTGCATATTTCCCAGAGTG
Tnfrsf1b	F: CCTGCCTACAAAGAGATGCCAAG
	R: GAACTGGGTGCTGTGGTCAAC
Kctd12	F: GCTGCTCTGGCGTATGTTCAC
	R: AGGATGTAGCGGAAGAGGAAGC
Acod1	F: CCTGCTGCTGGCGTTCAAC
	R: ATCTCTTTGGTATGTCTTTGGCTTCC
Ccl5	F: TGCTGCTTTGCCTACCTCTCC
	R: TGGCGGTTCCTTCGAGTGAC
Rsad2	F: CTCTGTGAGCATAGTGAGCAATGG
	R: GTCGCAGGAGATAGCAAGAATGTC
Lyz1	F: ACTCCTCCTGCTTTCTGTCACTG
	R: CACGGTAGCCATCCATTCCATTC
Csf3	F: GCCATGCCAGCCTTCACTTC
	R: GCGAGCCGTCTCCAGGAAG
Wfdc17	F: GTCCCAAGCCTTCACCAGAAAG
	R: TTGCAGACATGACCACAGCTATTG
Oas11	F: GGAAGAAGCCAAGCACCATCAG
	R: GTACTCTGTTAGTCACACTCAGGTTAC
GAPDH	F: GGCAAATTCAACGGCACAGTCAAG
	R: TCGCTCCTGGAAGATGGTGATGG

2.5.6 Western blot

Cells were seeded into 6-well plates at a density of 1×10^6 cells per well and treated with FS or LPS at the concentrations indicated in Section 2.5.4. After 24 h, cells were collected and lysed using radio-immunoprecipitation assay (RIPA) buffer containing phenylmethylsulfonyl fluoride (PMSF). The extracted proteins were separated by SDS-PAGE on a 4%-20% gradient gel and subsequently transferred to a 0.22 μm PVDF membrane. The membrane was blocked with Biyotime QuickBlock™ Western Blocking Buffer for 30 min, followed by incubation with specific primary antibodies at 4 °C overnight under gentle agitation. After six washes with Tris-buffered saline containing Tween-20 (TBST), the membrane was incubated with an HRP-conjugated secondary antibody for 1 h and washed again as described. Protein bands were visualized using an electrochemical chemiluminescence (ECL) kit and imaged with a Bio-Rad image system. ImageJ (version 1.53q, Wayne Rasband and contributors, National Institutes of Health, Bethesda, MD, USA) was used for quantitative analysis.

2.5.7 RNA-seq

Total RNA was extracted from cell samples for transcriptome analysis. RNA concentration and purity were measured using a Nanodrop 2000 spectrophotometer, and integrity was assessed by agarose gel electrophoresis. After passing quality control, mRNA was enriched using magnetic beads coated with Oligo (dT) to capture polyA tails. The mRNA was fragmented in fragmentation buffer and then reverse-transcribed into cDNA. cDNA libraries were constructed through PCR amplification and subjected to high-throughput sequencing on an Illumina platform.

Differential expressed genes (DEGs) were identified using a false discovery rate (FDR) < 0.05 and a fold-change threshold exceeding 1.5. Gene Ontology (GO) enrichment analysis of DEGs was performed with Gene Ontology Analysis Tools (Goatools), and pathway enrichment analysis was conducted using the Kyoto Encyclopedia of Genes and Genomes (KEGG) database.

2.6 Data processing

All experiments were performed at least three independent replicates. Data are presented as mean ± standard deviation (SD). Statistical significance was determined by one-way analysis of variance (ANOVA) followed by Duncan's multiple range test using IBM SPSS Statistics 26. A *P*-value < 0.05 was considered statistically significant.

3. Results and discussion

3.1 Isolation and purification of polysaccharides

The extraction and purification process for polysaccharides from *S. hemiphyllum* is illustrated in Fig. 1A. The crude polysaccharide fraction F was obtained with a yield of 3.90% (w/w). Fraction F was further separated using a DEAE-52 anion-exchange column, yielding three distinct polysaccharide fractions—FD1, FD2, and FD3 (Fig. 1B) with respective yields (calculated relative to the weight of F) of 13.44 ± 0.29%, 21.64 ± 0.35%, and 12.72 ± 0.95%, respectively. Among these, FD2 exhibited the highest yield and was selected for additional purification using a Sephacryl S-300 column, resulting in a final fraction (FS) with a recovery rate of 80% (relative to FD2 weight; Fig. 1C). The unimodal elution profile suggests effective isolation of a dominant molecular weight species, though further characterization is necessary to confirm its purity.

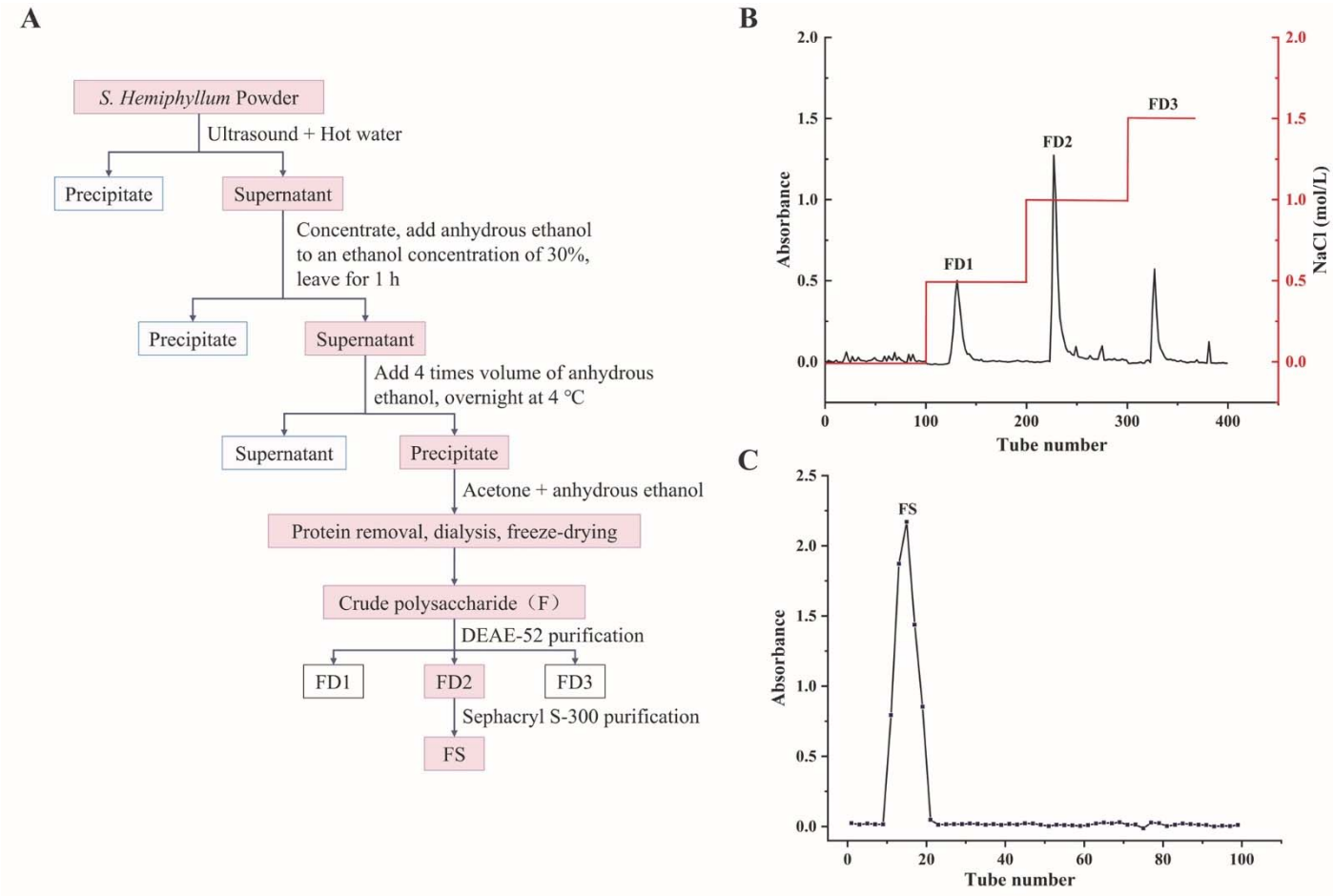

Fig. 1. Extraction and purification of fucoidan fractions. (A) Flowchart of extraction and purification of F. (B) Elution curve of F on DEAE-52. (C) Elution curve of FD2 on Sephacryl S-300.

3.2 Physiochemical Properties

3.2.1 Chemical composition and molecular weight

The basic chemical compositions of the crude polysaccharide (F) and its purified derivatives (FD2 and FS) are presented in Table 2. After two stages of purification, the total sugar content increased progressively: from 63.22 ± 0.59% in F, to 71.89 ± 0.38% in FD2, and 88.08 ± 2.05% in FS. Sulfate group contents were measured at 22.28 ± 0.75% for F, 14.86 ± 0.59% for FD2, and 18.83 ± 0.33% for FS. Protein content decreased across the purification steps, with values of 1.90 ± 0.12% (F), 1.49 ± 0.08% (FD2), and 1.12 ± 0.10% (FS). All three fractions contained minimal amounts of polyphenols, recorded at 1.82 ± 0.02% (F), 1.23 ± 0.01% (FD2), 1.22 ± 0.01% (FS).

The molecular weight distributions of F, FD2, and FS, as determined by refractive index detection, are shown in Fig. 2A-C. The peak molecular weights were 639.64 kDa for F, 389.14 kDa for FD2, and 373.14 kDa for FS, consistent with their heteropolysaccharide nature. The Mw of the crude polysaccharide in this study was notably lower than previously reported values for fucoidan (1166.48 kDa), which may be attributable to variations in raw material harvesting times (i.e., different years or seasons). Nevertheless, after purification, the polysaccharides obtained here exhibited higher molecular weights than those reported for fucoidans extracted from *Laminaria* species[31-32]. It has been suggested that lower molecular weight fucoidans possess improved solubility and absorption rates, which may enhance their immunomodulatory functions[33].

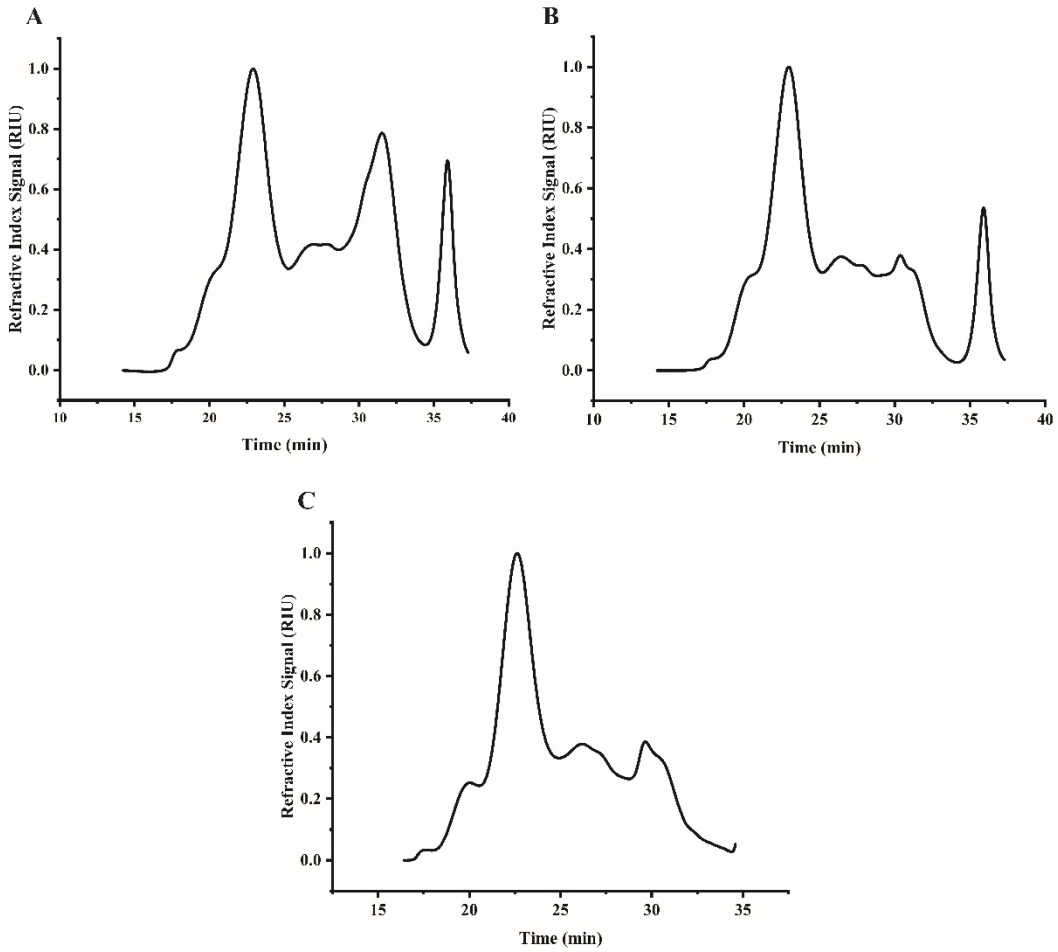

Fig. 2. Refractive index detector detection of F（A）、 FD2（B）、 FS（C）.

Table 2. Chemical composition and molecular weight of crude polysaccharide F, and purified polysaccharides FD2, FS.

Component	Total sugar (%)	Sulfate (%)	Polyphenol (%)	Protein (%)	Molecular weight (kDa)
F	63.22±0.59	22.28±0.75	1.82±0.02	1.90±0.12	639.64
FD2	71.89±0.38	14.86±0.59	1.23±0.01	1.49±0.08	389.14
FS	88.08±2.05	18.83±0.33	1.22±0.01	1.12±0.10	373.14

3.2.2 Monosaccharide composition

Understanding the structure and biological activity of polysaccharides requires detailed analysis of their monosaccharide composition[34]. Accordingly, the monosaccharide profiles of the crude polysaccharides (F) and two purified polysaccharides (FD2, and FS) were determined. As summarized in Fig.3 and Table 3, the major monosaccharide components of F were fucose (22.80%), galactose (15.40%), and glucuronic acid (15.95%). This profile differs from previously reported data, which showed higher glucose and lower glucuronic acid content in *S. hemiphyllum*-derived polysaccharides[19]; such differences may be attributed to variations between different batches of algal material.

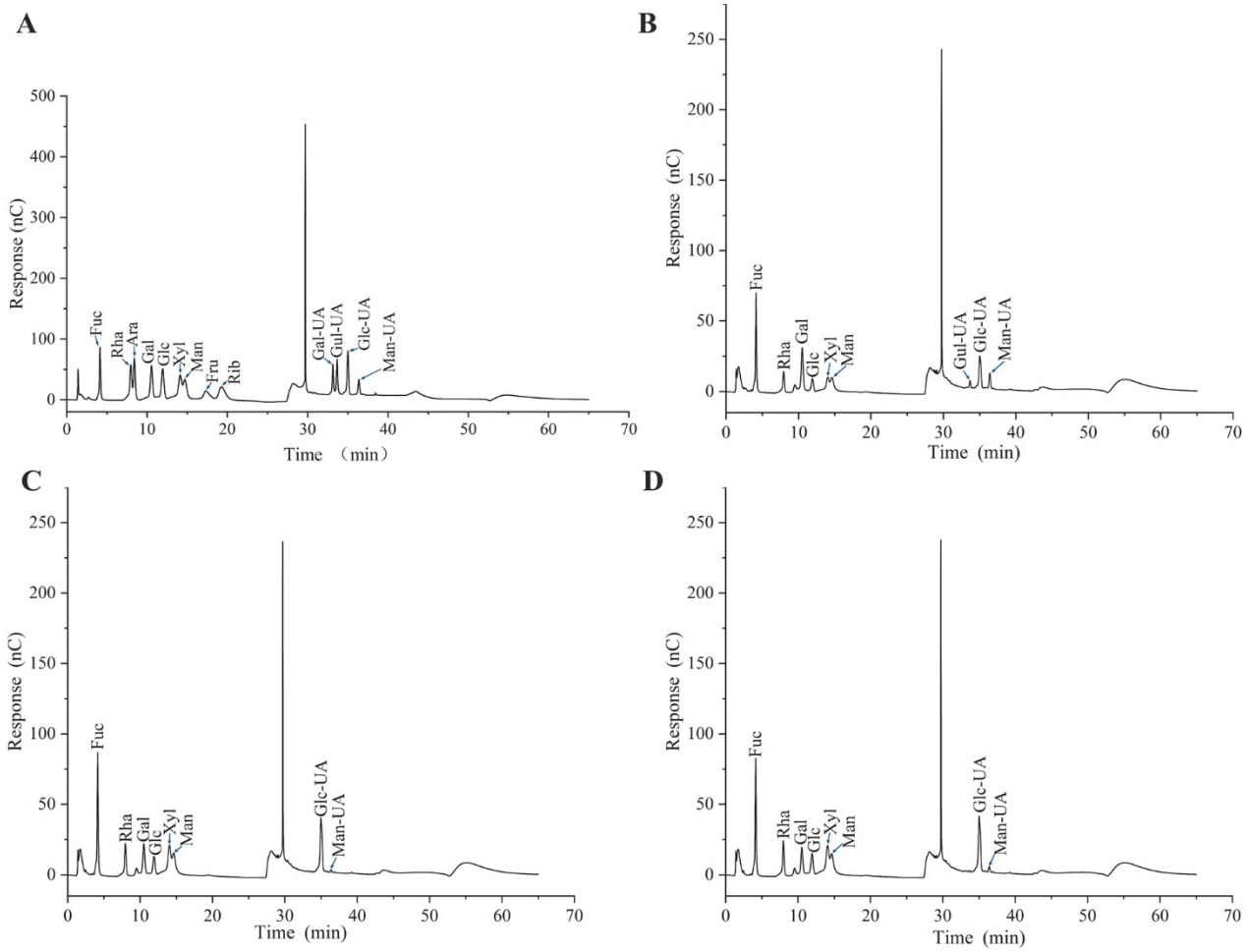

Fig. 3. Ion chromatogram of standard (A), crude polysaccharide F (B) and purified polysaccharide FD2 (C) and FS (D).

Table 3. Monosaccharide molar mass ratio of crude polysaccharide F, and purified polysaccharides FD2, FS.

Monosaccharide composition (molar ratio)	**F**	**FD2**	**FS**
Fucose (%)	22.80	24.51	23.00
Rhamnose (%)	5.64	8.23	8.96
Galactose (%)	15.40	9.10	7.91
Glucose (%)	4.58	5.55	6.50
Xylose (%)	7.42	13.07	12.36
Mannose (%)	11.09	13.91	13.39
Guluronic acid (%)	2.72	-	-
Glucuronic acid (%)	15.95	24.15	24.24
Mannuronic acid (%)	14.40	1.49	3.65

The main monosaccharides in both FD2 and FS were fucose (24.51% and 23.00%, respectively), mannose (13.91% and 13.39%), and glucuronic acid (24.15% and 24.24%). The high glucuronic acid content across all three samples indicates that these polysaccharides are acidic in nature. Notably, guluronic acid (2.72%), present in F, was absent in FD2 and FS, suggesting it may have been removed during the purification. Furthermore, the molar ratio of fucose to glucuronic acid in these fractions differed significantly from that reported for a fucoidan from *Sargassum thunbergii* purified using similar columns (DEAE-52 cellulose and the Sephacryl S-300), which exhibited a ratio of 8:1[35].

3.2.3 UV full wavelength scanning

As shown in Fig. 4A, the UV-vis absorption spectra of polysaccharides F, FD2, and FS were recorded between 200 and 600 nm. All three fractions exhibited weak absorption peaks at 260 nm and 280 nm, suggesting the presence of trace amounts of nucleic acids and proteins. This observation implies that these biomolecules may be difficult to remove completely from *S. sargassum* polysaccharides, possibly due to the formation of covalent glycoprotein complexes[36].

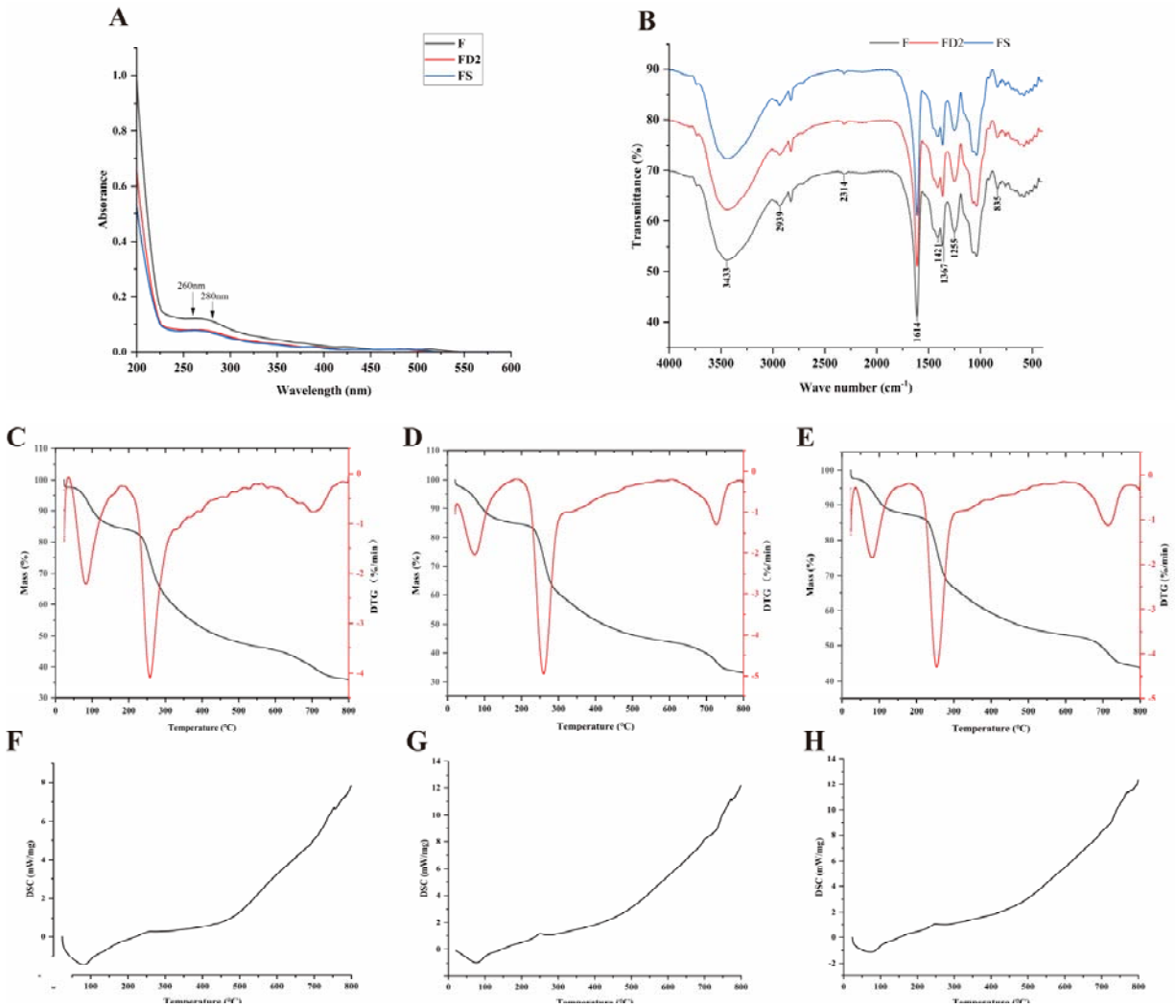

Fig. 4. Spectral analysis, thermal stability and morphological characteristics of F, FD2 and FS. (A) UV-vis spectra. (B) FT-IR spectra. (C) TG curve of F. (D) TG curve of FD2. (E) TG curve of FS. (F) DSC curve of F. (G) DSC curve of FD2. (H) DSC curve of FS.

3.2.4 FTIR

The FTIR spectra of all three polysaccharide fractions displayed characteristic absorption bands typical of polysaccharides (Fig. 4B). Overall, the spectral profiles were similar, indicating structural consistency between the crude and purified polysaccharides. A broad absorption band around 3433 cm^{-1} was attributed to O-H stretching vibrations. Peaks at 2939 cm^{-1}, 1421 cm^{-1}, and 1367 cm^{-1} were assigned to C-H stretching and bending vibrations. A weak signal at 2930-2940 cm^{-1} suggested the C-H stretching from the pyranoid ring and C6 groups of fucose[37-38]. The absorption at 1614 cm^{-1} corresponded to C=O stretching, likely from uronic acid residues[39-40]. The band at 1255 cm^{-1} indicated sulfate O=S=O stretching[41], while the absorption at

835 cm^{-1} was consistent with C-O-S bending vibrations[37]. The FTIR profile of FS showed similarities to those of commercial fucoidans[19] and fucoidan from other brown algae[38].

3.2.5 TG and DSC analysis

The thermal stability of polysaccharides was evaluated via TG-DSC analyses from 20 to 800 °C (Fig.4C-H). All three fractions exhibited three-stage weight loss patterns. The first region (23-183 °C) corresponded to the loss of free and bound water[42], with weight losses of 15.5% (F), 15.0% (FD2), and 12.7% (FS), indicating strong water retention capacity. The second stage (183-565 °C) involved major weight loss of 53.9% (F), 55.4% (FD2), and 46.2% (FS), likely due to polysaccharide decomposition[43]. The third stage (565-781 °C) may reflect further breakdown of complex molecular structures and inorganic residues[44].

DSC curves showed endothermic peaks at 84.31 °C (F), 77.24 °C (FD2) and 76.52 °C (FS), consistent with water evaporation and in agreement with TG results. The decomposition temperatures of all fractions were approximately 183 °C, aligning with previously reported thermal degradation temperatures of fucoidans (195 °C)[45], indicating good thermal stability.

3.2.6 SEM

SEM images at 200 × and 1000 × magnification revealed the surface morphologies of F, FD2, and FS (Fig. 5). Sample F exhibited irregular sheet- or block-like structures with rough edges. FD2 showed a porous surface with noticeable cavities, though with greater structural connectivity than F. In contrast, FS consisted mainly of irregular flakes with slightly curled edges.

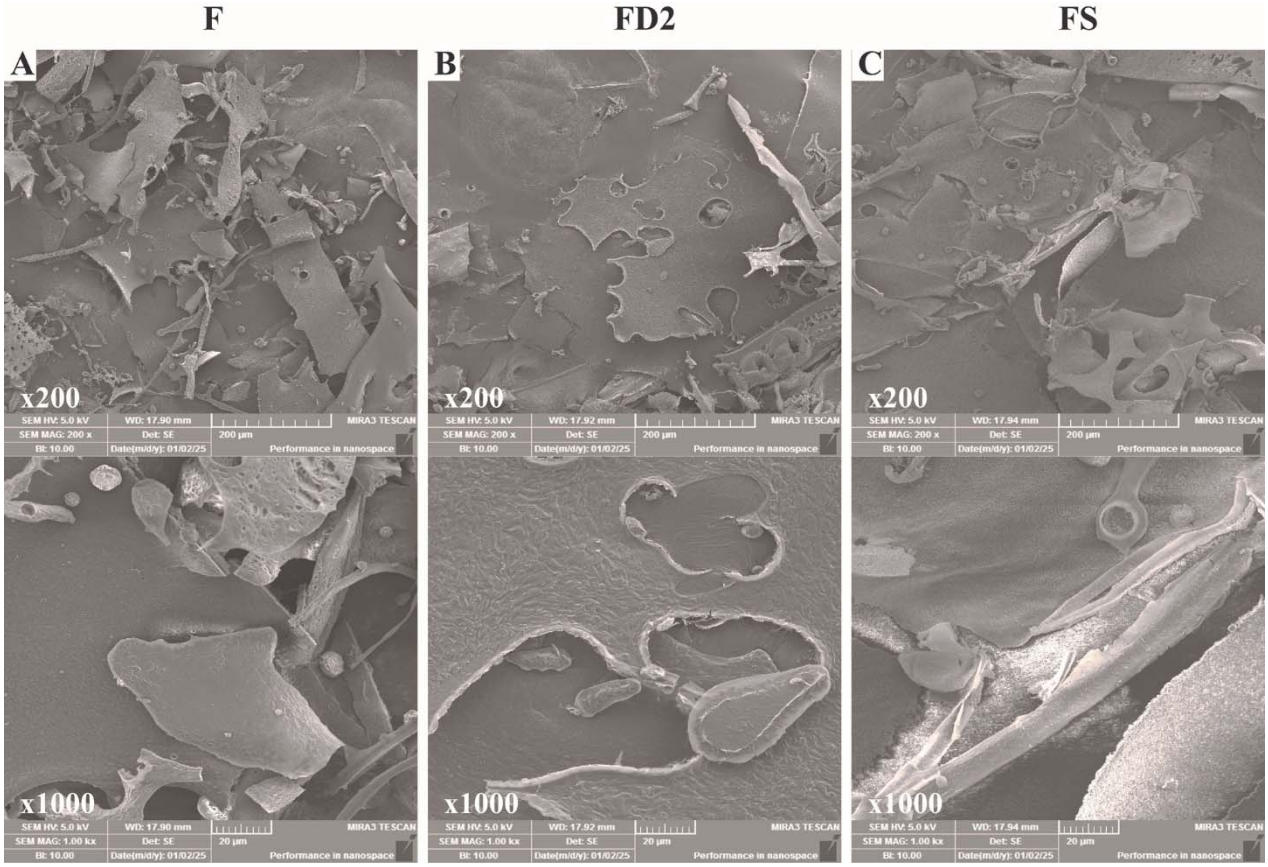

Fig. 5. (A) Morphological characteristics of F at (200 × and 1000 ×). (B) Morphological characteristics of FD2 at (200 × and 1000 ×). (C) Morphological characteristics of FS at (200 × and 1000 ×).

3.3 In vitro immunoreactivity

3.3.1 Effects of F, FD2, and FS on cell viability and NO release

The effects of F, FD2, and FS on the viability of RAW264.7 macrophages were evaluated using the CCK-8 assay. Cells were treated with different concentrations (6.25, 25, 100, and 200 μg/mL) of the polysaccharides or with LPS (1 μg/mL) as a positive control for 24 h. Compared to the control group, none of the polysaccharides at the tested concentrations showed significant cytotoxicity (Fig. 6A).

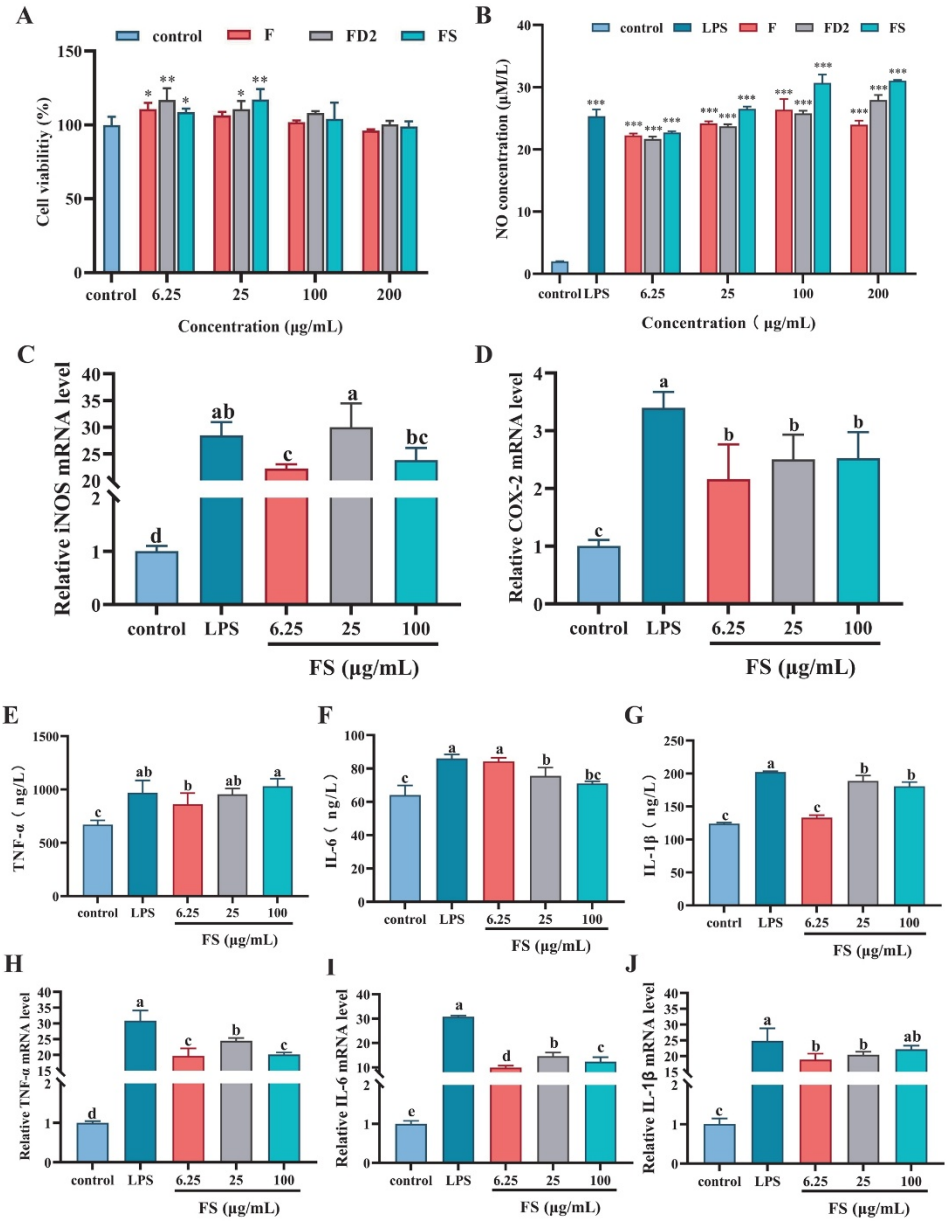

Fig. 6. Cytotoxicity and *in vitro* immune activity of F, FD2, and FS. (A) Effects of F, FD2, and FS on cell viability. (B) Effects of F, FD2, and FS on the release of NO.（C） The effect of FS on iNOS mRNA expression. (D) The effect of FS on COX-2 mRNA expression. Effect of FS on expression levels of cytokines TNF-α (E), IL-6 (F) and IL-1β（G）. Effect of FS on mRNA expression levels of cytokines TNF-α (H), IL-6 (I) and IL-1β (J). *$P < 0.05$, ** $P < 0.01$, and *** $P < 0.001$ compared to the control group. Bars with different letters are statistically different ($P < 0.05$). Bars with different letters are statistically different ($P < 0.05$).

NO is a key signaling molecule involved in macrophage functions such as antibacterial and antiviral responses, and plays important roles in various physiological and pathological processes. It also serves as a critical mediator in inflammation and immune regulation[46]. To assess the immunomodulatory effects of F,

FD2, and FS, NO production in the cell culture supernatant was measured. As shown in Fig. 6B, all three polysaccharides significantly promoted NO secretion at concentrations ranging from 6.25 to 200 μg/mL compared to the blank control. This observation is consistent with a report by Muthu et al., in which a low-molecular-weight fucoidan (25 kDa) from *Sargassum microcystum* showed the highest NO-inducing activity[47]. Therefore, FS was selected for further investigation. Moreover, since no significant difference in NO production was observed between 100 and 200 μg/mL of FS, the concentration range of 6.25-100 μg/mL was chosen for subsequent experiments.

3.3.2 Effect of FS on the gene expression levels of iNOS and COX-2

NO and PGE2 are key mediators in the immune response, synthesized by iNOS and COX-2, respectively[48-49]. We used RT-qPCR to evaluate the mRNA expression levels of iNOS and COX-2 in RAW264.7 cells after treatment with FS (Fig. 6C-D). Within the concentration range of 6.25 to 100 μg/mL, both iNOS and COX-2 mRNA levels were significantly up-regulated compared to the control group, though still markedly lower than those in the LPS-positive control group. This indicates that FS exerts a moderate immunostimulatory effect. Specifically, iNOS mRNA expression increased substantially as the FS concentration increased from 6.25 to 25 μg/mL. However, at 100 μg/mL, iNOS expression decreased compared to the level observed at 25 μg/mL. This biphasic response may reflect an autoregulatory mechanism whereby NO modulates NF-κB activity[50]. At lower concentrations, NO enhances iNOS expression, whereas beyond a certain threshold, it may exert inhibitory feedback. In the same concentration range, FS also promoted COX-2 mRNA expression, although the changes were not statistically significant. These findings demonstrate that FS can up-regulate the expression of genes associated with NO and PGE2 synthesis—namely iNOS and COX-2. Moreover, the interactions among these genes suggest their involvement in a coordinated immunomodulatory network, forming a complex molecular regulatory system during immune activation[51].

3.3.3 Effect of FS on the regulation of cytokine expression

To further investigate the immunomodulatory effects of polysaccharide FS, we quantified the secretion of TNF-α, IL-6, and IL-1β from RAW264.7 cells using ELISA following FS treatment. FS significantly enhanced the release of all three cytokines compared to the control (Fig. 6E-G). TNF-α and IL-1β levels increased across the concentration range without clear dose dependence. In contrast, IL-6 peaked at 6.25 μg/mL and decreased at higher concentrations. This non-monotonic response may result from receptor saturation, desensitization[52-53], activation of negative feedback mechanisms[54] or a shift in immune polarization[55]. This is similar to the concept proposed by Yu et al., who emphasized that the activity of polysaccharides is not a simple linear activation but involves a precise balancing process, often mediated through interactions with the host's mucosal environment[56].

3.3.4 Effect of FS on the regulation of cytokine gene expression

To further investigate the effect of FS on immune-related gene expression in RAW264.7 cells, the mRNA levels of TNF-α, IL-6, and IL-1β were quantitatively assessed using RT-qPCR after treatment with FS. As shown in Fig. 6 (H-J), FS significantly up-regulated the mRNA expression of TNF-α, IL-6, and IL-1β at concentrations ranging from 6.25 to100 μg/mL. Notably, the expression of TNF-α and IL-6 reached their peak when cells were treated with 25 μg/mL of FS, while the mRNA level of IL-1β showed no significant difference within the concentration range of 6.25-100 μg/mL.

3.4 Transcriptomic analysis of FS-treated RAW264.7 cells

3.4.1 Differentially expressed genes

To investigate the mechanism by which FS mediates immunomodulatory effects in macrophages, transcriptomics analysis was conducted on FS-treated cells. DEGs were identified using a threshold of multiple difference > 1.5 and FDR < 0.05 to assess significant expression differences between FS-treated and control groups. RT-qPCR analysis identified 501 differentially expressed genes (DGEs) in FS-treated RAW264.7 cells, inducing 206 up-regulated and 295 down-regulated genes (Fig. 7A). Validation by RT-qPCR of ten randomly selected DEGs confirmed the reliability of the transcriptomic data (Fig. 7B).

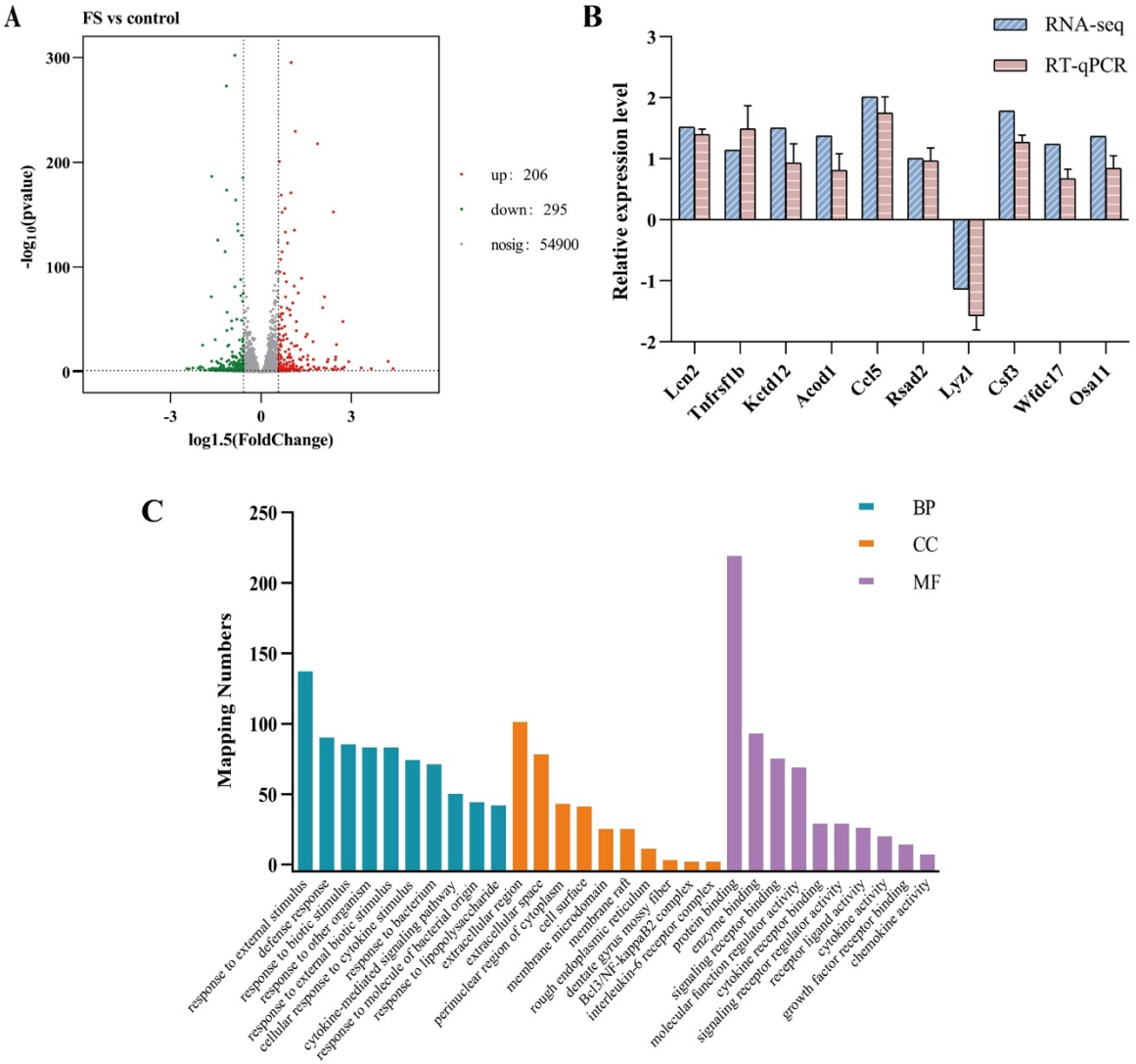

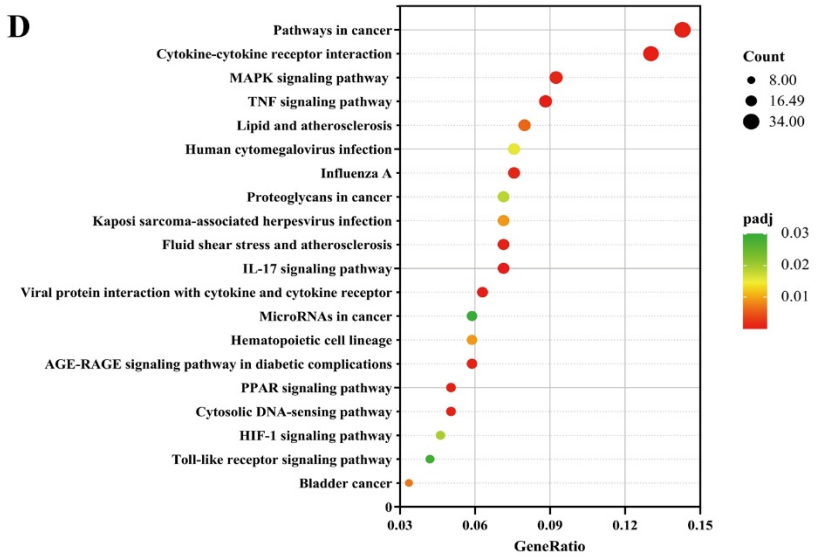

Fig. 7. Statistical plot of the number of differential genes between the FS group and the control group (A). Comparison of gene expression between RNA-Seq and RT-PCR (B). (C) Bubble diagram of GO enrichment analysis of DEGs. (D) Bubble plots of KEGG pathway enrichment analysis of DEGs.

3.4.2 GO enrichment and KEGG pathway analysis

To explore how FS regulates the biological mechanisms underlying macrophage immune function, we enriched and analyzed DEGs using the GO database. GO enrichment analysis assigned the DEGs to 571 biological processes (BP), 15 cellular component (CC), and 35molecular function (MF) terms (Fig. 7C). Top BP terms included “response to external stimulus”, “defense response” and “response to biotic stimulus”; CC terms included “extracellular region”, “extracellular space”, and “perinuclear region of cytoplasm”; and MF terms included “protein binding”, “enzyme binding”, and “signaling receptor binding”.

To elucidate the specific signaling pathways through which FS modulates immune functions in macrophages, KEGG functional annotation of DEGs between the FS-treated and control groups was conducted based on the KEGG database. The top 20 significantly enriched pathway are presented in Fig. 7D. KEGG enrichment analysis revealed that these pathways fell into three major categories: ten related to human diseases, five to organismal systems, and five to environmental information processing. Notably, several immune-related pathways such as the “MAPK signaling pathway”, “TNF signaling pathway”, “IL-17 signaling pathway”, and “Toll-like receptor signaling pathway” were significantly enriched. Among these, the TNF and IL-17 signaling pathways exhibited the most pronounced enrichment. These two pathways also shared a substantial number of commonly altered genes with close functional interrelationships, prompting their selection for further investigation. The enrichment of these immune-related pathways suggests that FS activates specific molecular mechanisms involved in immune responses, providing important insights and evidence for further understanding of immune physiological processes and related disease mechanisms.

3.4.3 Effect of FS on TNF/IL-17 signaling pathway in RAW264.7 macrophages

A close relationship exists between the TNF and IL-17 signaling pathways. Although IL-17 can independently induce the secretion of inflammatory factors, its effects are significantly enhanced upon synergy with TNF[57]. TNF-α, a key initiator of the TNF signaling pathway, plays a central role in regulating

immune cell functions, promoting inflammation responses, and maintaining immune homeostasis[58]. It binds to tumor necrosis factor receptors 1 or 2 (TNFR1 or TNFR2), triggering the recruitment of adaptor proteins such as TRAF1 and TRAF2[59]. The binding of TNF-α to TNFR2 is primarily associated with cell activation and proliferation, mainly through activation of the NF-κB signaling pathway. This results in the production of various inflammatory mediators, including TNF-α, IL-1β, and IL-6[60]. On the other hand, the IL-17 signaling pathway is critical for immune regulation and influences a wide range of immune responses, such as the initiation and maintenance of inflammation, and the activation and recruitment of immune cells[61]. Activation of the IL-17 pathway can also indirectly induce the NF-κB signaling pathway, thereby triggering the production of inflammatory factors[62].

Following the analysis of FS at the transcriptional level and in combination with transcriptomic results, we further examined key proteins associated with the TNF/IL-17 signaling pathways using Western blotting. As shown in Fig. 8(A-B), the expression levels of COX-2, iNOS, p65, p-p65, IL-6, as well as TNFR2 and TNF-α, were assessed. The results indicate that FS treatment markedly up-regulated the protein expression of TNF-α and its receptor TNFR2 in a concentration-dependent manner. This up-regulation was accompanied by increased expression of iNOS, COX-2, and IL-6. A noteworthy finding is that FS treatment elevated the level of p-p65 protein while concurrently accompanied by a decrease in total p65 protein. This seemingly paradoxical phenomenon is likely the result of strong negative feedback regulation within the NF-κB pathway. Sustained NF-κB activation induces the expression of various negative feedback regulators, including inhibitor of κB alpha (IκBα) and tumor necrosis factor alpha-induced protein 3 (A20)[63-64]. Among these, A20 can upstream regulate signaling by inhibiting IκB kinase (IKK) complex activity[64], while newly synthesized IκBα can shuttle p65 out of the nucleus back to the cytoplasm and inactivate it[65]. More importantly, strong signaling may have triggered the ubiquitin-proteasome degradation pathway of p65 protein itself[66], leading to the observed reduction in its total protein level. This suggests that the immunomodulatory effect of FS on macrophages is not a simple linear activation but involves a precise and dynamic balancing process. While receiving activation signals, cells also initiate self-protection mechanisms to prevent excessive inflammatory responses. This bidirectional regulatory mechanism also highlights the unique value of polysaccharides as immunomodulators. However, this interpretation requires further experimental confirmation. Techniques such as proteomics and microbiota analysis could help elucidate the underlying mechanisms[67]. Certain polysaccharides are known to enhance immune cell recognition and cytotoxicity while also modulating inflammatory signaling pathways to suppress excessive immune responses, thereby exerting bidirectional immunomodulatory effects[68]. Collectively, these findings suggest that FS activates the TNF and IL-17 signaling pathways, enhancing macrophage-mediated immunoregulation. The concomitant downregulation of NF-κB pathway components (p65 and p-p65) may indicate a regulatory feedback mechanism that prevents overactivation of inflammatory responses.

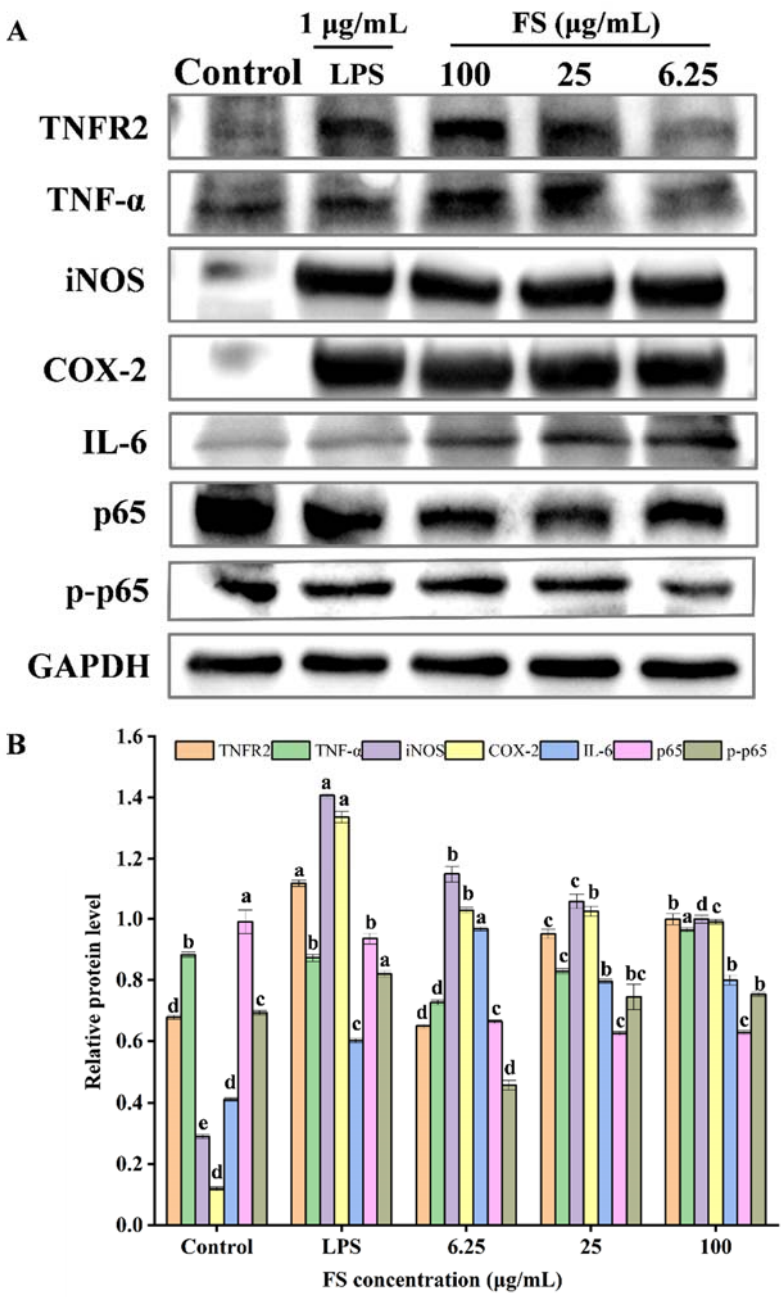

Fig.8. Effect of FS on the expression of related proteins in the TNF/IL-17 signaling pathways. Different letters indicate the significant differences between different treatments of the same protein ($P < 0.05$).

4. Conclusion

In this study, we isolated and purified a sulfated polysaccharide (FS) from *S. hemiphyllum* and systematically investigated its physicochemical properties and immunomodulatory effects. FS has a molecular weight of FS is 373.14 kDa and is primarily composed of fucose, galactose and glucuronic acid. However, due to its structural complexity and high molecular weight, more refined separation and purification techniques are required for further structural elucidation. Our results demonstrated that FS significantly enhanced the production of NO and the secretion of pro-inflammatory cytokines including TNF-α, IL-1β, and IL-6 in RAW264.7 macrophages, confirming that purification enhances its immunostimulatory activity. Transcriptomic analysis revealed 501 DEGs in response to FS treatment, among which 206 were up-regulated while 295 were down-regulated. Integrated transcriptomic and Western blot analyses indicated that FS

activates the TNF/IL-17 signaling pathways, thereby promoting immunoregulatory functions. These findings suggest that FS possesses significant immunoregulatory properties and shows promise as an effective immune modulator. We demonstrate that FS enhances immune responses in normal macrophages primarily through TNF/IL-17 pathways. However, the use of a heterogeneous fucoidan extract (FS) rather than a purified homogeneous fraction prevents us from establishing a precise structure-activity relationship. In addition, while this study provides mechanistic insight into its therapeutic potential, future research using immuno-compromised models is essential to advance translational applications. Subsequent in vivo animal studies and clinical trials will be necessary to validate the therapeutic relevance of *S. hemiphyllum*-derived polysaccharides. This work establishes *S. hemiphyllum* as a distinctive source of high-molecular-weight fucoidans with unique IL-17-mediated immunomodulation activity, contributing to both taxonomic specificity and pathway-focused innovation in marine polysaccharide research.

Acknowledgments

This work was funded by the Guangdong Basic and Applied Basic Research Foundation (2025A1515011519, 2023A1515011072), the Shenzhen Science and Technology Program (KCXFZ20240903094014019), the Special Funds for Universities in Guangdong Province in the Key Areas of Biomedicine and Health (2023ZDZX2025), the Postgraduate Education Innovation Project of Guangdong Ocean University (202438), the Program for Scientific Research Start-up Funds of Guangdong Ocean University (R20078, R19017), and the Innovative Team Program of High Education of Guangdong Province (2021KCXTD021). We Would like to thank Miss Xiuqiong Hou at Analytical and Testing Center of Guangdong Ocean University for the assistance with SEM imaging.

Declaration of Interest Statement

The authors declare that they have no known competing financial interests or personal relationships that could have appeared to influence the work reported in this paper.

References

[1] D. E. Place and T.-D. Kanneganti, The innate immune system and cell death in autoinflammatory and autoimmune disease, *Current Opinion in Immunology*, 2020, 67, 95-105. http://doi.org/10.1016/j.coi.2020.10.013

[2] D. Zhou, H. Zhang, X. Xue, Y. Tao, S. Wang, X. Ren and J. Su, Safety Evaluation of Natural Drugs in Chronic Skeletal Disorders: A Literature Review of Clinical Trials in the Past 20 years, *Frontiers in Pharmacology*, 2022, 12. http://doi.org/10.3389/fphar.2021.801287

[3] H. Zhang, J. Chen, Q. Zhang, L. Yu, X. Li and S. Wu, Oncogenic viral antigens for engineered T cell immunotherapy: Challenges and opportunities, *Medicine Advances*, 2023, 1, 306-317. http://doi.org/10.1002/med4.37

[4] M.-Y. Li, Q. Zhang, J. Li and G. Zengin, Food and medicine homology in cancer treatment: traditional thoughts collide with scientific evidence, *Food & Medicine Homology*, 2025, DOI: 10.26599/FMH.2025.9420120. http://doi.org/10.26599/FMH.2025.9420120

[5] C. Xie, Z. J. Lee, S. Ye, C. J. J. Barrow, F. R. R. Dunshea and H. A. R. Suleria, A Review on Seaweeds and Seaweed-Derived Polysaccharides: Nutrition, Chemistry, Bioactivities, and Applications, *Food Reviews International*, 2024, 40, 1312-1347. http://doi.org/10.1080/87559129.2023.2212055

[6] S. Nigam, R. Singh, S. K. Bhardwaj, R. Sami, M. P. Nikolova, M. Chavali and S. Sinha, Perspective on the Therapeutic Applications of Algal Polysaccharides, *Journal of Polymers and the Environment*, 2022, 30, 785-809. http://doi.org/10.1007/s10924-021-02231-1

[7] T. U. Jayawardena, L. Wang, K. K. A. Sanjeewa, S. I. Kang, J.-S. Lee and Y.-J. Jeon, Antioxidant Potential of Sulfated Polysaccharides from *Padina boryana*; Protective Effect against Oxidative Stress in In Vitro and In Vivo Zebrafish Model, *Marine Drugs*, 2020, 18. http://doi.org/10.3390/md18040212

[8] T. U. Jayawardena, I. P. S. Fernando, W. W. Lee, K. K. A. Sanjeewa, H.-S. Kim, D.-S. Lee and Y.-J. Jeon, Isolation and purification of fucoidan fraction in *Turbinaria ornata* from the Maldives; Inflammation inhibitory potential under LPS stimulated conditions in in-vitro and in-vivo models, *International Journal of Biological Macromolecules*, 2019, 131, 614-623. http://doi.org/10.1016/j.ijbiomac.2019.03.105

[9] M. El-Sheekh, E. A. Alwaleed, W. M. A. Kassem and H. Saber, Optimizing the fucoidan extraction using Box-Behnken Design and its potential bioactivity, *International Journal of Biological Macromolecules*, 2024, 277. http://doi.org/10.1016/j.ijbiomac.2024.134490

[10] H. S. A. Koh, J. Lu and W. Zhou, Structural Dependence of Sulfated Polysaccharide for Diabetes Management: Fucoidan From *Undaria pinnatifida* Inhibiting α-Glucosidase More Strongly Than α-Amylase and Amyloglucosidase, *Frontiers in Pharmacology*, 2020, 11. http://doi.org/10.3389/fphar.2020.00831

[11] Y.-X. Wang, X.-L. Chen, K. Zhou, L.-L. Wang, Y.-Z. Zhong, J. Peng, B.-S. Ge, C.-T. Ho and C.-Y. Lu, Fucoidan dose-dependently alleviated hyperuricemia and modulated gut microbiota in mice, *Food & Medicine Homology*, 2025, DOI: 10.26599/FMH.2026.9420095. http://doi.org/10.26599/FMH.2026.9420095

[12] R.-B. Jia, Y. Wu, Y. Zhou, Q. Zheng and M. Tan, Structural characterization of an acidic polysaccharide from scagassum and its effect on shelf life of golden pompano fillets during cold storage, *International Journal of Biological Macromolecules*, 2025, 298. http://doi.org/10.1016/j.ijbiomac.2025.140012

[13] T. A. Kuznetsova, T. P. Smolina, I. D. Makarenkova, L. A. Ivanushko, E. V. Persiyanova, S. P. Ermakova, A. S. Silchenko, T. S. Zaporozhets, N. N. Besednova, L. N. Fedyanina and S. P. Kryzhanovsky, Immunoadjuvant Activity of Fucoidans from the Brown Alga *Fucus evanescens*, *Marine Drugs*, 2020, 18. http://doi.org/10.3390/md18030155

[14] G. S. Anisha, S. Padmakumari, A. K. Patel, A. Pandey and R. R. Singhania, Fucoidan from Marine Macroalgae: Biological Actions and Applications in Regenerative Medicine, Drug Delivery Systems and Food Industry, *Bioengineering-Basel*, 2022, 9. http://doi.org/10.3390/bioengineering9090472

[15] R. Xian, R. Yang, P. Zhang, W. Chen, Q. Luo, J. Chen and H. Chen, Carotenoid Differences and Genetic Diversity in Populations of *Sargassum hemiphyllum* and *Sargassum fusiforme*, *Molecular Biotechnology*, 2023, 65, 1378-1386. http://doi.org/10.1007/s12033-022-00644-4

[16] B. Luo, Z. Wang, J. Chen, X. Chen, J. Li, Y. Li, R. Li, X. Liu, B. Song, K.-L. Cheong and S. Zhong, Physicochemical Characterization and Antitumor Activity of Fucoidan and Its Degraded Products from *Sargassum hemiphyllum* (Turner) C. Agardh, *Molecules*, 2023, 28. http://doi.org/10.3390/molecules28062610

[17] B.-R. Chen, W.-M. Li, T.-L. Li, Y.-L. Chan and C.-J. Wu, Fucoidan from *Sargassum hemiphyllum* inhibits infection and inflammation of *Helicobacter pylori*, *Scientific Reports*, 2022, 12. http://doi.org/10.1038/s41598-021-04151-5

[18] C.-Y. Huang, C.-H. Kuo and P.-W. Chen, Compressional-Puffing Pretreatment Enhances Neuroprotective Effects of Fucoidans from the Brown Seaweed *Sargassum hemiphyllum* on 6-Hydroxydopamine-Induced Apoptosis in SH-SY5Y Cells, *Molecules*, 2018, 23. http://doi.org/10.3390/molecules23010078

[19] R. Li, Q.-L. Zhou, S.-T. Chen, M.-R. Tai, H.-Y. Cai, R. Ding, X.-F. Liu, J.-P. Chen, L.-X. Luo and S.-Y. Zhong, Chemical Characterization and Immunomodulatory Activity of Fucoidan from *Sargassum hemiphyllum*, *Marine Drugs*, 2023, 21. http://doi.org/10.3390/md21010018

[20] K. Eswar, S. Mukherjee, P. Ganesan and A. K. Rengan, Immunomodulatory natural polysaccharides: An overview of the mechanisms involved, *European Polymer Journal*, 2023, 188. http://doi.org/10.1016/j.eurpolymj.2023.111935

[21] Z. Zhang, X.-M. Li, Y. Guo, H. Wang, Z. Li and H. Lin, Insight into the anti-allergic impacts of fucoidan from *Gracilaria lemaneiformis* in mitigating allergic reactions induced by shrimp tropomyosin via regulating Th1/Th2 cytokines and T cell subsets, *International Journal of Biological Macromolecules*, 2025, 299. http://doi.org/10.1016/j.ijbiomac.2025.140228

[22] G. M. Jose and G. M. Kurup, The efficacy of sulfated polysaccharides from *Padina tetrastromatica* in modulating the immune functions of RAW 264.7 cells, *Biomedicine & Pharmacotherapy*, 2017, 88, 677-683. http://doi.org/10.1016/j.biopha.2017.01.094

[23] D. Bi, B. Yu, Q. Han, J. Lu, W. L. White, Q. Lai, N. Cai, W. Luo, L. Gu, S. Li, H. Xu, Z. Hu, S. Nie and X. Xu, Immune Activation of RAW264.7 Macrophages by Low Molecular Weight Fucoidan Extracted from New Zealand *Undaria pinnatifida*, *Journal of Agricultural and Food Chemistry*, 2018, 66, 10721-10728. http://doi.org/10.1021/acs.jafc.8b03698

[24] S. Bahramzadeh, M. Tabarsa, S. You, C. Li and S. Bita, Purification, structural analysis and mechanism of murine macrophage cell activation by sulfated polysaccharides from *Cystoseira indica*, *Carbohydrate Polymers*, 2019, 205, 261-270. http://doi.org/10.1016/j.carbpol.2018.10.022

[25] Y. Wu, J. Liu, H. Hao, L. Hu, X. Zhang, L. Luo, J. Zeng, W. Zhang, I. N. Wong and R. Huang, A new polysaccharide from *Caulerpa chemnitzia* induces molecular shifts of immunomodulation on macrophages RAW264.7, *Food Chemistry-X*, 2022, 14. http://doi.org/10.1016/j.fochx.2022.100313

[26] K. Jiang, Y. Xu, Y. Wang, N. Yin, F. Huang and M. Chen, Unveiling the role of IL-17: Therapeutic insights and cardiovascular implications, *Cytokine & Growth Factor Reviews*, 2024, 77, 91-103. http://doi.org/10.1016/j.cytogfr.2024.05.001

[27] R. Li, Q.-L. Zhou, R.-Y. Yang, S.-T. Chen, R. Ding, X.-F. Liu, L.-X. Luo, Q.-Y. Xia, S.-Y. Zhong, Y. Qi and R. J. Williams, Determining the potent immunostimulation potential arising from the heteropolysaccharide structure of a novel fucoidan, derived from *Sargassum Zhangii*, *Food Chemistry-X*, 2023, 18. http://doi.org/10.1016/j.fochx.2023.100712

[28] I. Ogura, M. Sugiyama, R. Tai, H. Mano and T. Matsuzawa, Optimization of microplate-based phenol-sulfuric acid method and application to the multi-sample measurements of cellulose nanofibers, *Analytical Biochemistry*, 2023, 681. http://doi.org/10.1016/j.ab.2023.115329

[29] K. S. Dodgson and R. G. Price, A note on the determination of the ester sulphate content of sulphated polysaccharides, *The Biochemical journal*, 1962, 84, 106-110. http://doi.org/10.1042/bj0840106

[30] L. Veronica Pacheco, J. Parada, J. Ricardo Perez-Correa, M. Salome Mariotti-Celis, F. Erpel, A. Zambrano and M. Palacios, Bioactive Polyphenols from Southern Chile Seaweed as Inhibitors of Enzymes for Starch Digestion, *Marine Drugs*, 2020, 18. http://doi.org/10.3390/md18070353

[31] E.-K. An, J. Hwang, S.-J. Kim, H.-B. Park, W. Zhang, J.-H. Ryu, S. You and J.-O. Jin, Comparison of the immune activation capacities of fucoidan and laminarin extracted from *Laminaria japonica*, *International Journal of Biological Macromolecules*, 2022, 208, 230-242. http://doi.org/10.1016/j.ijbiomac.2022.03.122

[32] S. Li, W. Liu, Y. Li, X. Che, P. Xiao, S. Liu, Y. Ma, D. Ren, L. Wu, Q. Wang and Y. He, Extraction, purification, structural characterization and anti-hyperlipidemia activity of fucoidan from *Laminaria digitata*, *International Journal of Biological Macromolecules*, 2024, 279. http://doi.org/10.1016/j.ijbiomac.2024.135223

[33] Y. Zhao, L. Ning, P. Zhu, J. Jiang, Z. Yao and B. Zhu, The Origin, Properties, Structure, Catalytic Mechanism, and Applications of Fucoidan-Degrading Enzymes, *Marine Drugs*, 2025, 23, 97. http://doi.org/10.3390/md23030097

[34] D. Liu, W. Tang, J.-Y. Yin, S.-P. Nie and M.-Y. Xie, Monosaccharide composition analysis of polysaccharides from natural sources: Hydrolysis condition and detection method development, *Food Hydrocolloids*, 2021, 116. http://doi.org/10.1016/j.foodhyd.2021.106641

[35] M. Ou, X. Sun, J. Liang, F. Liu, L. Wang, X. Wu and J. Tu, A polysaccharide from *Sargassum thunbergii* inhibits angiogenesis *via* downregulating MMP-2 activity and VEGF/HIF-1α signaling, *International Journal of Biological Macromolecules*, 2017, 94, 451-458. http://doi.org/10.1016/j.ijbiomac.2016.10.046

[36] H. Zhang, R. J. Cotter and G. Editors, Glycoproteomics: new technology developments and applications provide renewed interest in glycoproteins. *Clinical Proteomics*, 2008, 4, 1-4.

[37] W. J. Kim, Y.-K. Koo, M.-K. Jung, H. R. Moon, S. M. Kim, A. Synytsya, H. S. Yun-Choi, Y. S. Kim, J. K. Park and Y. I. Park, Anticoagulating Activities of Low-Molecular Weight Fuco-Oligosaccharides Prepared by Enzymatic Digestion of Fucoidan from the Sporophyll of Korean *Undaria pinnatifida*, *Archives of Pharmacal Research*, 2010, 33, 125-131. http://doi.org/10.1007/s12272-010-2234-6

[38] S. Palanisamy, M. Vinosha, T. Marudhupandi, P. Rajasekar and N. M. Prabhu, Isolation of fucoidan from *Sargassum polycystum* brown algae: Structural characterization, *in vitro* antioxidant and anticancer activity, *International Journal of Biological Macromolecules*, 2017, 102, 405-412. http://doi.org/10.1016/j.ijbiomac.2017.03.182

[39] G. Chen, N. Jiang, J. Zheng, H. Hu, H. Yang, A. Lin, B. Hu and H. Liu, Structural characterization and anti-inflammatory activity of polysaccharides from Astragalus membranaceus, *International Journal of Biological Macromolecules*, 2023, 241. http://doi.org/10.1016/j.ijbiomac.2023.124386

[40] Y. Han, Y. Wu, G. Li, M. Li, R. Yan, Z. Xu, H. Lei, Y. Sun, X. Duan, L. Hu and R. Huang, Structural characterization and transcript-metabolite correlation network of immunostimulatory effects of sulfated polysaccharides from green alga *Ulva pertusa*, *Food Chemistry*, 2021, 342. http://doi.org/10.1016/j.foodchem.2020.128537

[41] Z. Zhang, H. Wang, T. Chen, H. Zhang, J. Liang, W. Kong, J. Yao, J. Zhang and J. Wang, Synthesis and structure characterization of sulfated galactomannan from fenugreek gum, *International Journal of Biological Macromolecules*, 2019, 125, 1184-1191. http://doi.org/10.1016/j.ijbiomac.2018.09.113

[42] E.-J. Go and K. Bin Song, *Capsosiphon fulvescens* films containing persimmon (*Diospyros kaki* L.) leaf extract, *Food Bioscience*, 2020, 37. http://doi.org/10.1016/j.fbio.2020.100723

[43] A. Abuduwaili, P. Mutailifu, R. Nuerxiati, Y. Gao, H. A. Aisa and A. Yili, Structure and biological activity of polysaccharides from *Nitraria sibirica* pall fruit, *Food Bioscience*, 2021, 40. http://doi.org/10.1016/j.fbio.2021.100903

[44] F. Wu and H. Huang, Surface morphology and protective effect of *Hericium erinaceus* polysaccharide on cyclophosphamide-induced immunosuppression in mice, *Carbohydrate Polymers*, 2021, 251. http://doi.org/10.1016/j.carbpol.2020.116930

[45] R. M. Rodriguez-Jasso, I. Ortiz, S. I. Mussatto, L. Pastrana, C. N. Aguilar and J. A. Teixeira, Optimization of sulphated polysaccharides recovery from brown seaweeds by microwave-assisted extraction, *Journal of Biotechnology*, 2010, 150, S394-S395. http://doi.org/10.1016/j.jbiotec.2010.09.508

[46] E. M. Palmieri, C. McGinity, D. A. Wink and D. W. McVicar, Nitric Oxide in Macrophage Immunometabolism: Hiding in Plain Sight, *Metabolites*, 2020, 10. http://doi.org/10.3390/metabo10110429

[47] S. Muthu, A. B. Altemimi, M. Lakshmikanthan, K. Krishnan, Q. H. ALKaisy, F. H. Awlqadr and M. A. Hesarinejad, Phycocolloids from *Sargassum microcystum*: Immunomodulatory and antioxidant activities of alginic acid and fucoidan, *Food Hydrocolloids for Health*, 2025, 7, 100209. http://doi.org/10.1016/j.fhfh.2025.100209

[48] A. Kulesza, L. Paczek and A. Burdzinska, The Role of COX-2 and PGE2 in the Regulation of Immunomodulation and Other Functions of Mesenchymal Stromal Cells, *Biomedicines*, 2023, 11. http://doi.org/10.3390/biomedicines11020445

[49] M. A. Cinelli, H. T. Do, G. P. Miley and R. B. Silverman, Inducible nitric oxide synthase: Regulation, structure, and inhibition, *Medicinal Research Reviews*, 2020, 40, 158-189. http://doi.org/10.1002/med.21599

[50] P. A. Vo, B. Lad, J. A. P. Tomlinson, S. Francis and A. Ahluwalia, Autoregulatory role of endothelium-derived nitric oxide (NO) on lipopolysaccharide-induced vascular inducible NO synthase expression and function, *Journal of Biological Chemistry*, 2005, 280, 7236-7243. http://doi.org/10.1074/jbc.M411317200

[51] D. Salvemini, S. F. Kim and V. Mollace, Reciprocal regulation of the nitric oxide and cyclooxygenase pathway in pathophysiology: relevance and clinical implications, *American Journal of Physiology-Regulatory Integrative and Comparative Physiology*, 2013, 304, R473-R487. http://doi.org/10.1152/ajpregu.00355.2012

[52] V. Capra, M. R. Accomazzo, F. Gardoni, S. Barbieri and G. E. Rovati, A role for inflammatory mediators in heterologous desensitization of $CysLT_1$ receptor in human monocytes, *Journal of Lipid Research*, 2010, 51, 1075-1084. http://doi.org/10.1194/jlr.M003236

[53] M. Li, M. Wang, Y. Wen, H. Zhang, G.-N. Zhao and Q. Gao, Signaling pathways in macrophages: molecular mechanisms and therapeutic targets, *MedComm*, 2023, 4, e349-e349. http://doi.org/10.1002/mco2.349

[54] T. Hirano, IL-6 in inflammation, autoimmunity and cancer, *International Immunology*, 2021, 33, 127-148. http://doi.org/10.1093/intimm/dxaa078

[55] L. A. Belfield, J. H. Bennett, W. Abate and S. K. Jackson, Exposure to *Porphyromonas gingivalis* LPS during macrophage polarisation leads to diminished inflammatory cytokine production, *Archives of Oral Biology*, 2017, 81, 41-47. http://doi.org/10.1016/j.archoralbio.2017.04.021

[56] Y.-Y. Yu, Y.-N. Duan, S. Ma, Q.-H. Hu and G.-X. Ma, Research progress on the mechanism of functional activity of edible fungi polysaccharides—focusing intestinal mucus as a key and entry point, *Food & Medicine Homology*, 2025, 2, 9420042. http://doi.org/10.26599/FMH.2025.9420042

[57] M. I. Koenders, L. A. B. Joosten and W. B. van den Berg, Potential new targets in arthritis therapy: interleukin (IL)-17 and its relation to tumour necrosis factor and IL-1 in experimental arthritis, *Annals of the rheumatic diseases*, 2006, 65 Suppl 3, iii29-33. http://doi.org/10.1136/ard.2006.058529

[58] P. Saha and A. Smith, TNF-α (Tumor Necrosis Factor-): A Paradox in Thrombosis, *Arteriosclerosis Thrombosis and Vascular Biology*, 2018, 38, 2542-2543. http://doi.org/10.1161/atvbaha.118.311660

[59] S. Naserian, M. E. Abdelgawad, M. A. Bakshloo, G. Ha, N. Arouche, J. L. Cohen, B. L. Salomon and G. Uzan, The TNF/TNFR2 signaling pathway is a key regulatory factor in endothelial progenitor cell immunosuppressive effect, *Cell Communication and Signaling*, 2020, 18. http://doi.org/10.1186/s12964-020-00564-3

[60] A. Ruiz, Y. Palacios, I. Garcia and L. Chavez-Galan, Transmembrane TNF and Its Receptors TNFR1 and TNFR2 in Mycobacterial Infections, *International Journal of Molecular Sciences*, 2021, 22. http://doi.org/10.3390/ijms22115461

[61] R. M. Onishi and S. L. Gaffen, Interleukin-17 and its target genes: mechanisms of interleukin-17 function in disease, *Immunology*, 2010, 129, 311-321. http://doi.org/10.1111/j.1365-2567.2009.03240.x

[62] H. Liu, S. Yuan, K. Zheng, G. Liu, J. Li, B. Ye, L. Yin and Y. Li, IL-17 signaling pathway: A potential therapeutic target for reducing skeletal muscle inflammation, *Cytokine*, 2024, 181. http://doi.org/10.1016/j.cyto.2024.156691

[63] T. Lawrence, The nuclear factor NF-κB pathway in inflammation, *Cold Spring Harbor perspectives in biology*, 2009, 1, a001651. http://doi.org/10.1101/cshperspect.a001651

[64] S.-C. Sun, The non-canonical NF-κB pathway in immunity and inflammation, *Nature reviews immunology*, 2017, 17, 545-558. http://doi.org/10.1038/nri.2017.52

[65] T. Liu, L. Zhang, D. Joo and S.-C. Sun, NF-κB signaling in inflammation, *Signal transduction and targeted therapy*, 2017, 2, 1-9. http://doi.org/10.1038/sigtrans.2017.23

[66] S. Ghosh and M. Karin, Missing pieces in the NF-κB puzzle, *cell*, 2002, 109, S81-S96. http://doi.org/10.1016/s0092-8674(02)00703-1

[67] Q. Liang, Q. Zhao, X. Hao, J. Wang, C. Ma, X. Xi and W. Kang, The Effect of *Flammulina velutipes* Polysaccharide on Immunization Analyzed by Intestinal Flora and Proteomics, *Frontiers in Nutrition*, 2022, 9. http://doi.org/10.3389/fnut.2022.841230

[68] P. P. Bhuyan, R. Nayak, S. Patra, H. S. Abdulabbas, M. Jena and B. Pradhan, Seaweed-derived sulfated polysaccharides; the new age chemopreventives: a comprehensive review, *Cancers*, 2023, 15, 715. http://doi.org/10.3390/cancers15030715